Copyright © 2015 Tech Science Press CMES, vol.105, no.5, pp.341-360, 2015

A Second-order Time-marching Procedure with Enhanced Accuracy

Delfim Soares Jr.[1]

Abstract: In this work, a second-order time-marching procedure for dynamics is discussed, in which enhanced accuracy is enabled. The new technique is unconditionally stable (according to its parameter selection), it has no amplitude decay or overshooting, and it provides reduced period elongation errors. The method is based on displacement-velocity relations, requiring no computation of accelerations. It is efficient, simple and very easy to implement. Numerical results are presented along the paper, illustrating the good performance of the proposed technique. As it is described here, the new method has no drawbacks when compared to the Trapezoidal Rule (TR), which is one of the most popular time-marching techniques in dynamics, being always more accurate than the TR.

Keywords: Time Integration Methods, Trapezoidal Rule, Central Difference Method, Stability, Accuracy, Period Elongation Errors.

1 Introduction

Time dependent hyperbolic equations have numerous applications in various branches of science and in practical engineering design. Since it is usually very difficult to obtain analytical transient responses for these equations, numerical techniques must be applied to find approximate solutions, and step-by-step time integration algorithms are routinely employed when dynamic problems are focused, because of their various inherent advantages to solve a great deal of initial value problems.

The literature reports many classical explicit [Tamma and Namburu (1990); Hulbert and Chung (1996) etc.] and implicit [Newmark (1959); Chung and Hulbert (1993) etc.] algorithms for time-marching analysis (for a comprehensive review, see Tamma et al., 2000). Explicit procedures are usually preferable because of their lower computational effort, being the restrictions due to stability conditions their

[1] Structural Engineering Department, Federal University of Juiz de Fora, CEP 36036-330, Juiz de Fora, MG, Brazil. E-mail: delfim.soares@ufjf.edu.br

main disadvantage. Implicit approaches, on the other hand, can be settled unconditionally stable, being characterized, however, by higher computational costs. Many procedures can be employed to improve stability and accuracy of time-integration algorithms, such as subcycling techniques [Smolinski (1996); Soares et al. (2007); Casadei and Halleux (2009)], high-order accurate schemes [Fung (2002); Mancussi and Ubertini (2003)], automatic time step control [Hulbert and Jang (1995); Rossi et al. (2014)] etc. As a matter of fact, a lot of research is continuously realized on this field and several time-marching techniques are available nowadays for dynamic and wave propagation analyses [Bathe (2007); Chang (2010); Soares (2011, 2015); Elgohary et al. (2014a,b) etc.].

Amongst explicit time integration methods, the nearly universal choice is the Central Difference Method (CD). Amongst implicit approaches, the Trapezoidal Rule (TR), or Constant Average Acceleration Method, is probably the most widely used technique. More elaborate schemes have been proposed, which require larger implicit systems or more implicit systems of the size of the stiffness and mass to be solved at each step, and improved properties have been obtained. However, these techniques require considerable higher storage and computational effort and thus have not been widely adopted. As a matter of fact, it can be considered that for a method to be competitive, no more than one set of standard implicit equations should have to be solved at each time step [Hughes (2000)].

In this work, an improved second-order time-marching technique is proposed. The methodology is based on an intermediate behavior between the TR and the CD, in a way that unconditional stability can be always ensured and reduced period elongation errors are obtained. Thus, enhanced accuracy is provided by the new technique. Moreover, the proposed method is only based on single-step displacements-velocities relations, being truly self-starting and very simple to implement. Along the paper, numerical results are presented, illustrating the good performance of the method.

2 Governing equations and time integration strategy

The governing system of equations describing a linear dynamic model is given by [Clough and Penzien (1993)]:

$$\mathbf{M}\ddot{\mathbf{U}}(t)+\mathbf{C}\dot{\mathbf{U}}(t)+\mathbf{K}\mathbf{U}(t)=\mathbf{F}(t) \tag{1}$$

where $\mathbf{M}$, $\mathbf{C}$ and $\mathbf{K}$ are mass, damping and stiffness matrices, respectively, $\mathbf{F}(t)$ stands for the force vector and $\mathbf{U}(t), \dot{\mathbf{U}}(t)$ and $\ddot{\mathbf{U}}(t)$ are displacement, velocity and acceleration vectors, respectively. The initial conditions of the model are given by:

$$\mathbf{U}^0=\mathbf{U}(0) \tag{2a}$$

$$\dot{\mathbf{U}}^0 \;= \dot{\mathbf{U}}(0) \tag{2b}$$

where $\mathbf{U}^0$ and $\dot{\mathbf{U}}^0$ stand for initial displacement and velocity vectors, respectively.

By time integrating the equation of motion (1), considering a time-step Δt, one may write:

$$\mathbf{M}\int_{t-\frac{\Delta t}{2}}^{t+\frac{\Delta t}{2}} \ddot{\mathbf{U}}(\tau)d\tau + \mathbf{C}\int_{t-\frac{\Delta t}{2}}^{t+\frac{\Delta t}{2}} \dot{\mathbf{U}}(\tau)d\tau + \mathbf{K}\int_{t-\frac{\Delta t}{2}}^{t+\frac{\Delta t}{2}} \mathbf{U}(\tau)d\tau = \int_{t-\frac{\Delta t}{2}}^{t+\frac{\Delta t}{2}} \mathbf{F}(\tau)d\tau \tag{3}$$

which may be viewed as a simple weighted residual form of the governing equation.

The integrals in the l.h.s. of equation (3) may be approximated by:

$$\Im_{\ddot{\mathbf{U}}}^{n+\frac{1}{2}} = \int_{t-\frac{\Delta t}{2}}^{t+\frac{\Delta t}{2}} \ddot{\mathbf{U}}(\tau)d\tau \approx \dot{\mathbf{U}}^{n+1} - \dot{\mathbf{U}}^{n} \tag{4a}$$

$$\Im_{\dot{\mathbf{U}}}^{n+\frac{1}{2}} = \int_{t-\frac{\Delta t}{2}}^{t+\frac{\Delta t}{2}} \dot{\mathbf{U}}(\tau)d\tau \approx \mathbf{U}^{n+1} - \mathbf{U}^{n} \tag{4b}$$

$$\Im_{\mathbf{U}}^{n+\frac{1}{2}} = \int_{t-\frac{\Delta t}{2}}^{t+\frac{\Delta t}{2}} \mathbf{U}(\tau)d\tau \approx \Delta t\,\mathbf{U}^{n} + \tfrac{1}{2}(1-\alpha)\Delta t^2\dot{\mathbf{U}}^{n} + \tfrac{1}{2}\alpha\,\Delta t^2\dot{\mathbf{U}}^{n+1} \tag{4c}$$

where $\mathbf{U}^n$, $\dot{\mathbf{U}}^n$ and $\ddot{\mathbf{U}}^n$ are the approximations of $\mathbf{U}(t^n)$, $\dot{\mathbf{U}}(t^n)$ and $\ddot{\mathbf{U}}(t^n)$, respectively, $t^n = n\Delta t$, and α is an integration parameter for the method. The displacement $\mathbf{U}^{n+1}$ can be defined by the following simple finite difference expression:

$$\mathbf{U}^{n+1} \;= \mathbf{U}^{n} + \tfrac{1}{2}\Delta t\,\dot{\mathbf{U}}^{n} + \tfrac{1}{2}\Delta t\,\dot{\mathbf{U}}^{n+1} \tag{5}$$

Taking into account approximations (4) and (5), equation (3) may be rewritten as the following recursive relation:

$$(\mathbf{M} + \tfrac{1}{2}\Delta t\,\mathbf{C} + \tfrac{1}{2}\alpha\,\Delta t^2\mathbf{K})\,\dot{\mathbf{U}}^{n+1} = \Im_{\mathbf{F}}^{n+\frac{1}{2}} + \mathbf{M}\dot{\mathbf{U}}^{n} - \tfrac{1}{2}\Delta t\,\mathbf{C}\dot{\mathbf{U}}^{n} - \mathbf{K}(\Delta t\,\mathbf{U}^{n} + \tfrac{1}{2}(1-\alpha)\Delta t^2\dot{\mathbf{U}}^{n}) \tag{6}$$

where $\Im_{\mathbf{F}}^{n+\frac{1}{2}}$ stands for the integral in the r.h.s. of equation (3).

Equation (6) enables to compute the velocities $\dot{\mathbf{U}}^{n+1}$, and equation (5) may then be used to compute the displacements at the current time step. It is important to highlight that the method described by equations (5) and (6) is a single-step method based only on velocities and displacements, being no computation of accelerations required. Thus, the first positive feature of the method is that it is truly self-starting, eliminating any kind of cumbersome initial procedure, such as the computation of initial accelerations (which usually requires an extra system of equations to be dealt with) and/or the computation of multistep initial values.

As it is discussed in the next section, the present formulation is second-order accurate. For $\alpha = 1/2$, the TR is reproduced. Thus, an unconditionally stable technique is obtained, without amplitude decay and with positive period elongation. For $\alpha = 0$, the basic features of the CD are reproduced. Thus, a conditionally stable technique arises, which enables no amplitude decay and produces negative period elongation (once its critical limit is not reached). For $0 < \alpha < 1/2$, the method is conditionally stable (with its critical limit, which is function of α, always higher than that of the CD), it has no amplitude decay and its period elongation errors are intermediary between the TR and the CD. Thus, if stability is ensured, more accurate results may be obtained by $0 < \alpha < 1/2$ than by $\alpha = 0$ or $\alpha = 1/2$, since period elongation errors are reduced.

The strategy here is to select $0 < \alpha < 1/2$ in a way that stability is always ensured. Then, an unconditionally stable technique can be obtained, which is more accurate than the TR due to reduced period elongation errors. In order to do so, the following expression for α may be adopted:

$$\alpha = \frac{1}{2}\tanh(a\omega\Delta t) \tag{7}$$

where a stands as a control parameter. Considering a proper selection of a, the method is unconditionally stable. As it is described in the next section, this proper selection is given by $a \geq a_c$, where $a_c = 0.24567002$ (rounded value) is the critical value of a. One should observe that the TR is reproduced by $a = \infty$; thus, the present formulation should always provide more accurate results than the TR, once $a \geq a_c$ is selected.

In equation (7), ω represents the maximal natural frequency of the model. This value does not need to be precisely computed, since a can always be selected a bit higher than its critical value ($a = 0.25$ is recommended here). Thus, ω can be simply estimated, so that the efficiency of the technique is not compromised.

3 Properties of the method

In this section, the single-degree-of-freedom (SDOF) problem is considered in order to discuss the properties (i.e., stability, accuracy etc.) of the proposed methodology, following standard guidelines [Hughes (2000); Bathe (1996)]. The equation of motion for the SDOF model can be written as:

$$\ddot{u}(t) + 2\xi w\dot{u}(t) + w^2u(t) = f(t) \tag{8}$$

where ξ is the damping ratio and w is the natural frequency of the model. Considering equation (8) and the proposed methodology, the following recursive relationship can be written:

$$\begin{bmatrix} u^{n+1} \\ \dot{u}^{n+1} \end{bmatrix} = \begin{bmatrix} A_{11} & A_{12} \\ A_{21} & A_{22} \end{bmatrix} \begin{bmatrix} u^{n} \\ \dot{u}^{n} \end{bmatrix} + \begin{bmatrix} L_{11} & L_{12} & L_{13} \\ L_{21} & L_{22} & L_{23} \end{bmatrix} \begin{bmatrix} f^{n} \\ f^{n+\frac{1}{2}} \\ f^{n+1} \end{bmatrix} = \mathbf{A} \begin{bmatrix} u^{n} \\ \dot{u}^{n} \end{bmatrix} + \mathbf{L} \begin{bmatrix} f^{n} \\ f^{n+\frac{1}{2}} \\ f^{n+1} \end{bmatrix} \tag{9}$$

where **A** and **L** stand for the amplification and the load operator matrices, respectively.

In the new procedure, the amplification matrix **A** is given by equations (10):

$$A_{11} = [1 + \xi\, w\Delta t + \tfrac{1}{2}(\alpha - 1)w^2\Delta t^2]/A_0 \tag{10a}$$

$$A_{12} = [1 + \tfrac{1}{4}(2\alpha - 1)w^2\Delta t^2]\,\Delta t/A_0 \tag{10b}$$

$$A_{21} = [-w^2\Delta t^2]\,(1/\Delta t)/A_0 \tag{10c}$$

$$A_{22} = [1 - \xi\, w\Delta t + \tfrac{1}{2}\alpha\, w^2\Delta t^2]/A_0 \tag{10d}$$

where $A_0 = 1 + \xi\, w\Delta t + \frac{1}{2}\alpha\, w^2\Delta t^2$; or by equations (11), if relation (7) is considered:

$$A_{11} = [1 + \xi\, w\Delta t + \tfrac{1}{4}(\tanh(a\omega\Delta t) - 2)w^2\Delta t^2]/A_0 \tag{11a}$$

$$A_{12} = [1 + \tfrac{1}{4}(\tanh(a\omega\Delta t) - 1)w^2\Delta t^2]\,\Delta t/A_0 \tag{11b}$$

$$A_{21} = [-w^2\Delta t^2]\,(1/\Delta t)/A_0 \tag{11c}$$

$$A_{22} = [1 - \xi\, w\Delta t + \tfrac{1}{4}\tanh(a\omega\Delta t)w^2\Delta t^2]/A_0 \tag{11d}$$

where $A_0 = 1 + \xi\, w\Delta t + \frac{1}{4}\tanh(a\omega\Delta t)\, w^2\Delta t^2$.

The load operator matrix **L** may be given by:

$$L_{11} = \tfrac{1}{2}\beta_1\, \Delta t^2/A_0 \tag{12a}$$

$$L_{12} = \tfrac{1}{2}\beta_2\, \Delta t^2/A_0 \tag{12b}$$

$$L_{13} = \tfrac{1}{2}\beta_3\, \Delta t^2/A_0 \tag{12c}$$

$$L_{21} = \beta_1\, \Delta t/A_0 \tag{12d}$$

$$L_{22} = \beta_2\, \Delta t/A_0 \tag{12e}$$

$$L_{23} = \beta_3\, \Delta t/A_0 \tag{12f}$$

where β_1, β_2 and β_3 are integration parameters. These parameters can be selected, for instance, as $\beta_1 = \beta_3 = 1/4$ and $\beta_2 = 1/2$, if the trapezoidal rule is followed (in this case, the term 'trapezoidal rule' stands for the quadrature rule for approximating integrals, and not for the time marching procedure), or as $\beta_1 = \beta_3 = 1/6$ and $\beta_2 = 2/3$, if the Simpson rule is followed. If linear behaviour is assumed for the load within Δt, the load integration parameters can be simply selected as $\beta_1 = \beta_3 = 1/2$ and $\beta_2 = 0$.

By analyzing the amplification and load operator matrices, one can notice that the TR can be reproduced by adopting $\alpha = 1/2$ (or $a = \infty$) and $\beta_1 = \beta_3 = 1/2$ and $\beta_2 = 0$. Thus, the new technique allows to select more accurate load operators than the TR, if necessary.

3.1 Convergence

The expansion of the amplification matrix (11) in Taylor's series is given by:

$$A_{11} = 1 - \tfrac{1}{2}w^2\Delta t^2 + \tfrac{1}{2}\xi\, w^3\Delta t^3 + O(\Delta t^4) \tag{13a}$$

$$A_{12} = \Delta t - \xi\, w\Delta t^2 - \tfrac{1}{4}(1-4\xi^2)\, w^2\Delta t^3 + O(\Delta t^4) \tag{13b}$$

$$A_{21} = -w^2\Delta t + \xi\, w^3\Delta t^2 - \xi^2 w^4\Delta t^3 + O(\Delta t^4) \tag{13c}$$

$$A_{22} = 1 - 2\xi\, w\Delta t - \tfrac{1}{2}(1-4\xi^2)\, w^2\Delta t^2 + \tfrac{1}{2}(\xi - 4\xi^3)\, w^3\Delta t^3 + O(\Delta t^4) \tag{13d}$$

By comparing it with the expansion of the analytical amplification matrix, which is given by:

$$A^a_{11} = 1 - \tfrac{1}{2}w^2\Delta t^2 + \tfrac{1}{3}\xi\, w^3\Delta t^3 + O(\Delta t^4) \tag{14a}$$

$$A^a_{12} = \Delta t - \xi\, w\Delta t^2 - \tfrac{1}{6}(1-4\xi^2)\, w^2\Delta t^3 + O(\Delta t^4) \tag{14b}$$

$$A^a_{21} = -w^2\Delta t + \xi\, w^3\Delta t^2 + \tfrac{1}{6}(1-4\xi^2)\, w^4\Delta t^3 + O(\Delta t^4) \tag{14c}$$

$$A^a_{22} = 1 - 2\xi\, w\Delta t - \tfrac{1}{2}(1-4\xi^2)\, w^2\Delta t^2 + \tfrac{2}{3}(\xi - 2\xi^3)\, w^3\Delta t^3 + O(\Delta t^4) \tag{14d}$$

one may observe that the method is second-order accurate.

3.2 Stability

The stability condition requires that matrix $\mathbf{A}$ does not amplify errors as the time-step algorithm advances on time. The conditions required to assure stability are [Hughes (2000); Bathe (1996)]: (i) $\rho(\mathbf{A}) \leq 1$; (ii) eigenvalues of $\mathbf{A}$ of multiplicity greater than one are strictly less than one in modulus. In item (i), $\rho(\mathbf{A})$ is the spectral radius of matrix $\mathbf{A}$, which represents the maximal absolute magnitude of the eigenvalues of $\mathbf{A}$.

The eigenvalues of the amplification matrix of the method in focus are given by equation (15), where A_1 is half the trace of matrix **A** and A_2 is the determinant of **A**, as defined by equations (16):

$$\lambda_{1,2}(\mathbf{A}) = A_1 \pm (A_1^2 - A_2)^{1/2} \tag{15}$$

$$A_1 = [1 + \tfrac{1}{2}(\alpha - 1)\Omega^2]/A_0 \tag{16a}$$

$$A_2 = [1 - \xi\,\Omega + \tfrac{1}{2}(1 + \alpha)\Omega^2]/A_0 \tag{16b}$$

where $\Omega = w\Delta t$ is the sampling frequency of the model.

By analyzing the spectral radius of matrix **A**, it can be established that the method is unconditionally stable for $\alpha \geq 1/2$. For $\alpha < 1/2$, the method is conditionally stable, and its critical sampling frequency is given by:

$$\Omega_c = (\tfrac{1}{4} - \tfrac{1}{2}\alpha)^{-1/2} \tag{17}$$

or, taking into account expression (7), by:

$$\Omega_c = \tfrac{1}{a} RootOf(\Omega^2 - 2e^{2\Omega}a^2 - 2a^2) \tag{18}$$

where the function *RootOf* indicates the root of its argument.

The a value at which $\Omega_c = \Omega$ (and thus the method is stable) is given by:

$$a_{\Omega_c} = \tfrac{1}{\Omega}\tanh^{-1}(1 - 4/\Omega^2) \tag{19}$$

which has a maximal value of:

$$a_c = \max(a_{\Omega_c}) = 0.24567002... \tag{20}$$

Thus, for $a \geq a_c$ one has $\Omega_c \geq \Omega$, and the method is always stable.

3.3 Accuracy

Taking into account the homogeneous SDOF model equation, velocities may be eliminated by repeated use of (9) to obtain a difference equation in terms of displacements, as follows:

$$u^{n+1} - 2A_1u^n + A_2u^{n-1} = 0 \tag{21}$$

Comparison of (21) with the characteristic equation of **A** indicates that the solution has the representation:

$$u^n = c_1\lambda_1^n + c_2\lambda_2^n \tag{22}$$

where the coefficients c_1 and c_2 are determined by the initial data and it is considered that $\lambda_1 \neq \lambda_2$. When λ_1 and λ_2 are complex conjugate, solution (22) can be compared to the undercritically-damped model solution

$$\bar{u}^n = \exp(-\bar{\xi}\,\bar{w}t^n)[\bar{c}_1 \cos(\bar{w}_D t^n) + \bar{c}_2 \sin(\bar{w}_D t^n)] \tag{23}$$

allowing to establish error measures.

Considering $\lambda_{1,2} = A \pm Bi$, $c_{1,2} = c_r \pm c_i i$ and $\bar{c}_{1,2} = \bar{c}_r \pm \bar{c}_i i$, the comparison of equations (22) and (23) provides:

$$(c_r \pm c_i i)(A \pm Bi)^n = (\bar{c}_r \pm \bar{c}_i i)\exp[(-\bar{\xi}\,\bar{w} \pm \bar{w}_D i)\Delta t\, n] \tag{24}$$

where:

$$c_r = \bar{c}_r = \tfrac{1}{2}u^0 \tag{25a}$$

$$c_i = \tfrac{1}{2}[(A - A_{11})/B]\,u^0 - \tfrac{1}{2}[A_{12}/B]\,\dot{u}^0 \tag{25b}$$

$$\bar{c}_i = \tfrac{1}{2}[-\xi\, w/w_D]\,u^0 - \tfrac{1}{2}[1/w_D]\,\dot{u}^0 \tag{25c}$$

By adopting the polar forms $A \pm Bi = \rho\exp(\pm\phi i)$, $c_r \pm c_i i = r\exp(\pm\theta i)$ and $\bar{c}_r \pm \bar{c}_i i = \bar{r}\exp(\pm\bar{\theta} i)$, equation (24) can be rewritten as:

$$(r/\bar{r})\rho^n \exp[(\pm\phi n \pm \theta \mp \bar{\theta})i] = \exp(-\bar{\xi}\,\bar{w}\Delta t\, n)\exp[(\pm\bar{w}_D \Delta t\, n)i] \tag{26}$$

From which one may define:

$$\bar{w}_D \Delta t = \phi + (\theta - \bar{\theta})/n \tag{27a}$$

$$\bar{\xi}\,\bar{w}\Delta t = -\ln(\rho) \tag{27b}$$

$$A_f = (r/\bar{r})^{1/n} \tag{27c}$$

which allows to compute period elongation, amplitude decay and amplitude factor error measures, respectively.

In Fig. 1, spectral radii, period elongation and amplitude decay measures are depicted, considering several values for a. In the present method, there is no overshooting nor amplitude decay, and $A_f = 1$ and $\bar{\xi} = 0$ are always obtained for $a \geq a_c$. In Fig. 2, a closer look at period elongation errors is depicted, taking into account the proposed technique (with $a = 0.25$), the TR, the CD and the two-step Bathe method [Bathe (2007); Bathe and Baig (2005)]. In Fig. 3, the relative errors (computed in the discrete L^2 norm) of an undamped unitary initial displacement model (i.e., $u^0 = 1$ and $\dot{u}^0 = 0$) are depicted (in this case, the analytical solution is given by $u(t) = \cos(wt)$). As one can observe in the figures, the new technique may considerably improve the accuracy of the analysis, reducing period elongation and providing overall reduced errors (one should keep in mind that the TR and the basic features of the CD are reproduced by $a = \infty$ and $a = 0$, respectively). As it is illustrated in Fig. 2, the proposed single-step technique can even provide more accurate results than some multistep techniques.

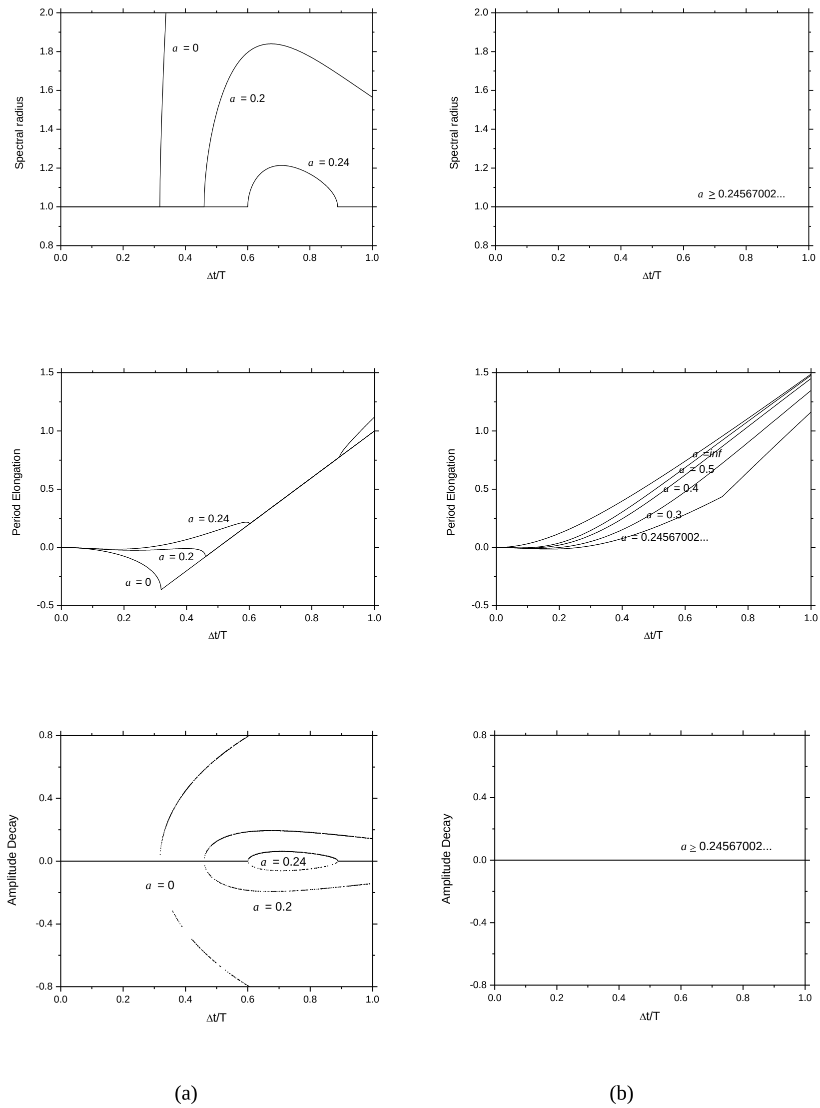

Figure 1: Spectral radius, period elongation and amplitude decay: (a) conditionally stable ($a < 0.24567002...$); (b) unconditionally stable ($a \geq 0.24567002...$).

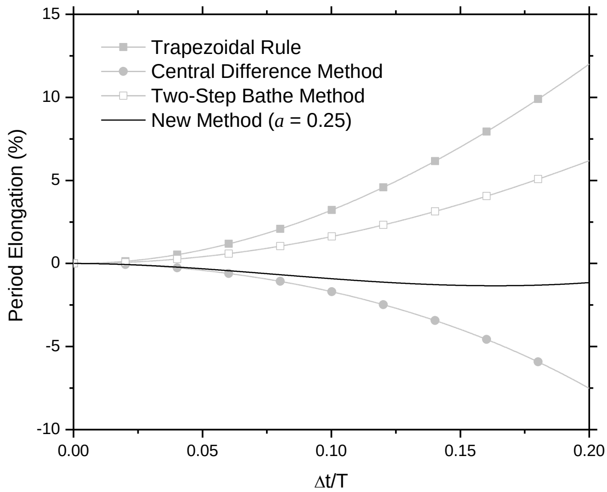

Figure 2: Period elongation considering different numerical methods.

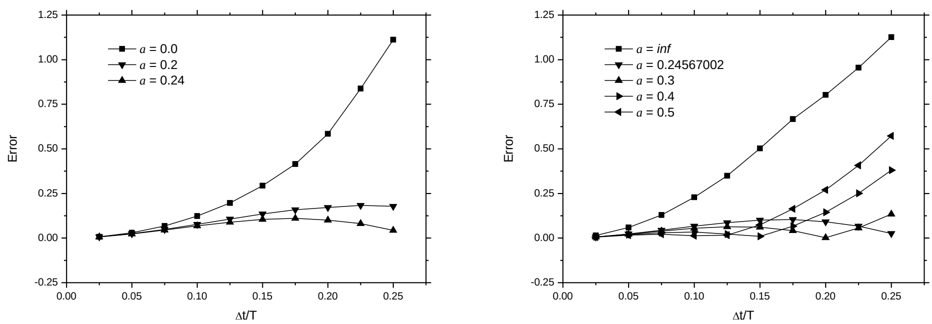

(a) (b)

Figure 3: Error vs. discretization: (a) conditionally stable ($a < 0.24567002...$); (b) unconditionally stable ($a \geq 0.24567002...$).

4 Numerical examples

In this section, three numerical examples are presented to further illustrate the superior accuracy of the proposed technique.

In the first application, the axial displacements of an elastic rod are analyzed, whereas, in the second application, the transversal motion of a square membrane is studied. Both the rod and the membrane models are spatially discretized by linear triangular finite elements and, for all the analyses that follow, $\beta_1 = \beta_3 = 1/2$ and $\beta_2 = 0$ are adopted. Unconditionally stable procedures are focused here, and $a = 0.25$ is always considered. These two examples aim to illustrate the superior accuracy of the new technique taking into account its amplification matrix. The obtained results are compared to those obtained by the TR and by the Bathe method [Bathe (2007); Bathe and Baig (2005)].

In the third application the possibility of enhanced accuracy due to a better load operator selection (which is enabled by the new method) is illustrated. In this case, explicit conditional stable techniques ($a = 0$) are focused, and results are compared to those obtained by the CD.

In the next two applications, a measure of the adopted time-step length is computed according to the following expression:

$$\varphi = c\Delta t/\ell \tag{28}$$

where $c$is the (primary) wave velocity and ℓ is the characteristic finite element length.

4.1 Rectangular rod

The first example is that of a rectangular body behaving like a one-dimensional rod [Soares and Mansur (2007)]. It is fixed at one end and subjected to a Heaviside type forcing function acting at its opposite end. A sketch of the model is shown in Fig. 4(a). The material properties of the rod are: $\nu = 0$ (Poisson's ratio); $E = 100 N/m^2$ (Young's modulus); and $\rho = 1.0 kg/m^3$ (mass density). The geometry of the model is defined by $L = 1\,m$. As depicted in Fig. 4(b), 320 finite elements are employed to spatially discretize the model. Regarding the temporal discretization, different time-steps are adopted, uniformly varying from $\Delta t = 6.25 \cdot 10^{-4}\,s$ $(\varphi = 0.25)$ to $\Delta t = 6.25 \cdot 10^{-3}\,s$ $(\varphi = 2.5)$.

For this model, analytical answers for the axial displacements are available, and they are expressed as:

$$u(x,t) = \frac{8PL}{E\pi^2} \sum_{n=1}^{\infty} \frac{(-1)^{n-1}}{(2n-1)^2} \sin\left(\frac{2n-1}{2L}\pi x\right)\left(1 - \cos\left(\frac{2n-1}{2L}\pi ct\right)\right) \tag{29}$$

where P stands for the amplitude of the applied load.

In spite of its geometrical and load simplicity, the present application represents a rather complex time-domain numerical computation, since successive reflections occur at the model extremities. These systematic multiple reflections can emphasize some numerical aspects, such as numerical instabilities and/or errors amplifications. In Fig. 5(a), relative error results (L^2norm) for the computed displacements

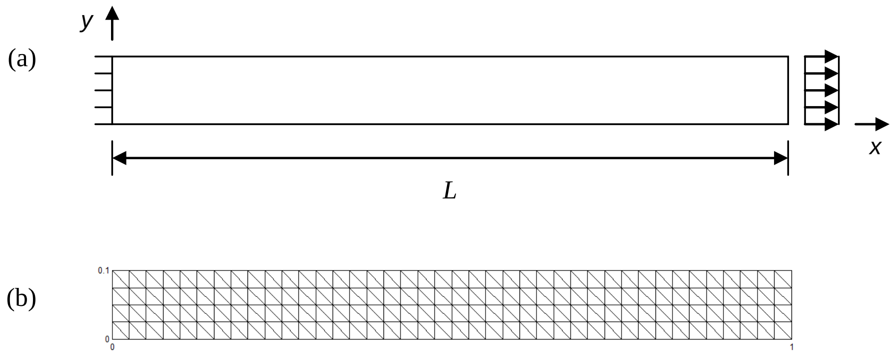

Figure 4: Sketch of the rod (a) and adopted finite element mesh (b).

at the middle of the rod are depicted, taking into account the proposed technique and the TR. As one can observe, considerably better accuracy is obtained by the proposed formulation. For instance, the computed error related to the new method and $\Delta t = 1.875 \cdot 10^{-3}\, s$ ($\varphi = 0.75$), is close to that obtained by the TR for a time-step three times smaller ($\varphi = 0.25$). In Fig. 5(b), relative error results are presented taking into account the proposed technique and the Bathe method. Since the Bathe method is a two-step time marching procedure, in order to present results related to equivalent computational demands, the errors of the proposed technique depicted in Fig. 5(b) are evaluated taking into account two applications of the method within a time-step. As one can observe in Fig. 5(b), the new technique provides much more accurate results than the Bathe method for the same computational effort. In fact, for the present application, even if a single-step approach is considered, regarding the proposed technique, it still provides more accurate results than the two-step Bathe method for $\varphi \leq 1$, as it is illustrated in Fig. 5. Thus, the proposed technique not only is very accurate, but also quite efficient, demanding very low computational effort to provide very good results.

4.2 Square membrane

The subject of this investigation is the transverse motion of a square membrane that has initial velocity prescribed over its central domain (grey area in Fig. 6(a)) and null displacements prescribed over its entire boundary [Mansur et al. (2004)]. The physical properties of the membrane are $c = 10\,m/s$ (wave velocity) and $\rho = 1.0\,kg/m^3$ (mass density). The geometry of the model is defined by $L = 10\,m$ and $l = 4\,m$. The symmetry of the membrane is considered and just 1/4 of it is discretized. The adopted finite element mesh is depicted in Fig. 6(b) (1250 elements are employed in the mesh).

(a)

(b)

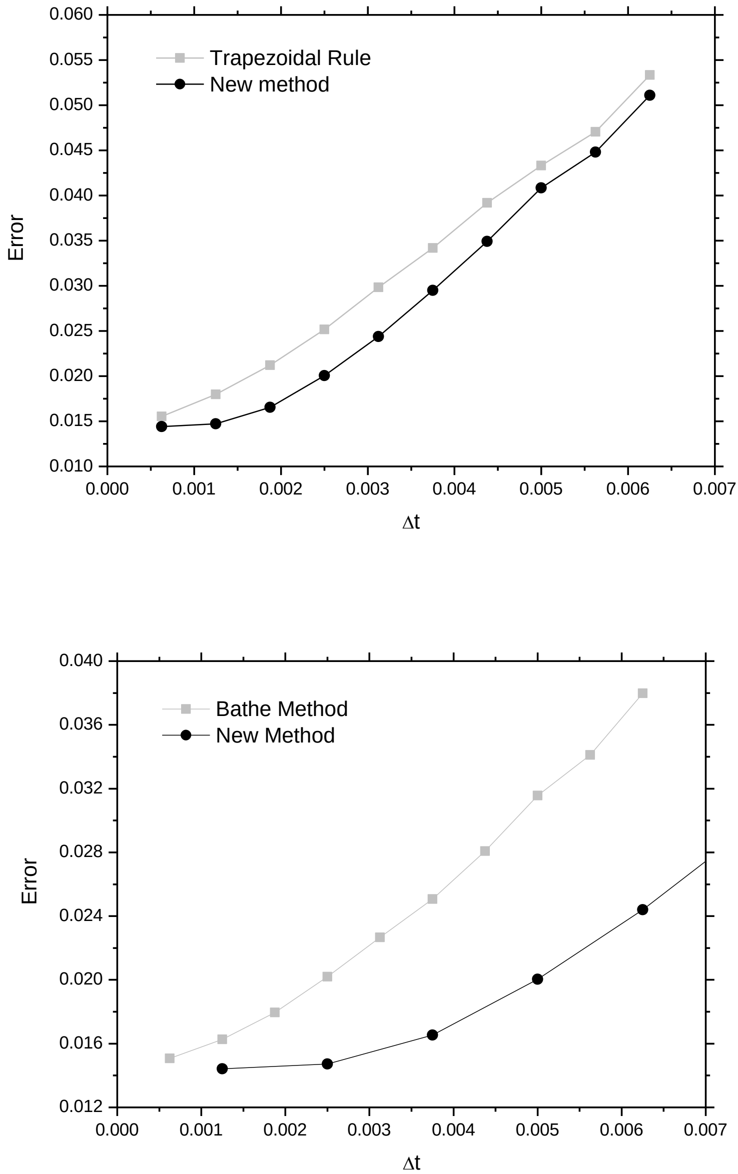

Figure 5: Error vs. time discretization for the rod: (a) single-step approach; (b) two-step approach.

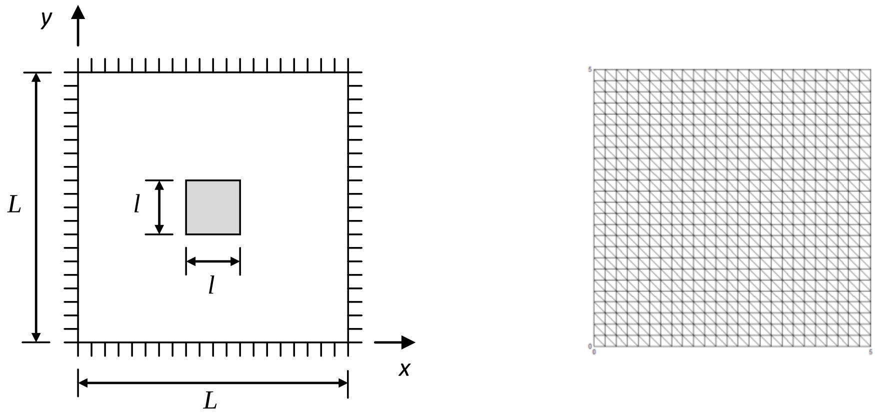

(a) (b)

Figure 6: Sketch of the membrane (a) and adopted finite element mesh (b).

For this model, analytical answers for the transversal displacements are available, and they are expressed as:

$$u(x,y,t)=\frac{4VL}{c\pi^3}\sum_{m=1}^{\infty}\sum_{n=1}^{\infty}\frac{C_{mn}}{mn(m^2+n^2)^{1/2}}\sin\left(\frac{m}{L}\pi x\right)\sin\left(\frac{n}{L}\pi y\right)\sin\left(\frac{(m^2+n^2)^{1/2}}{L}\pi ct\right) \tag{30}$$

where $C_{mn}=[\cos(0.7\pi m)-\cos(0.3\pi m)][\cos(0.7\pi n)-\cos(0.3\pi n)]$ and V stands for the amplitude of the applied initial velocity.

In Fig. 7, relative error results for the computed displacements at the middle of the membrane are depicted, taking into account different temporal discretizations (with φ varying uniformly from 0.25 to 2.5). Once again, as expected, the proposed technique provides better accuracy than the TR. In fact, as demonstrated in section 3, the proposed technique will always provide an enhanced performance.

In Fig. 8, results computed along the discretized membrane are depicted, taking into account 9 selected time instants (one should keep in mind that a relative poor spatial discretization is being considered here). As it can be observed, the wave propagation evolution becomes quite complex in the present application, with successive reflections and superposition of wave fronts taking place.

(a)

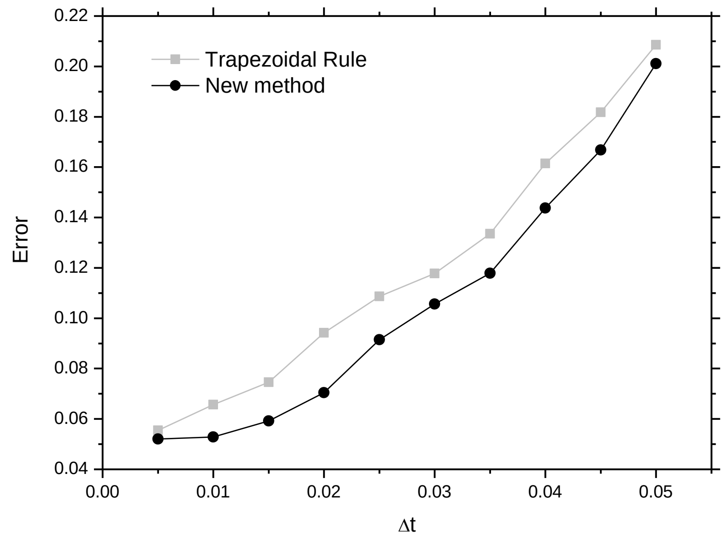

(b)

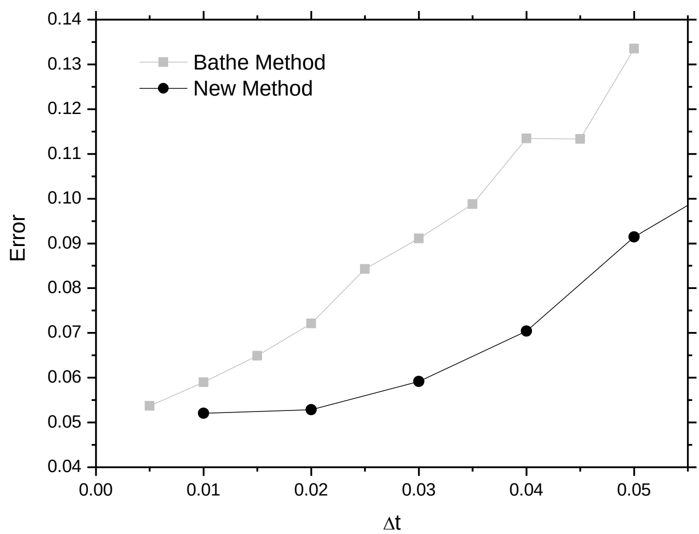

Figure 7: Error vs. time discretization for the membrane: (a) single-step approach; (b) two-step approach.

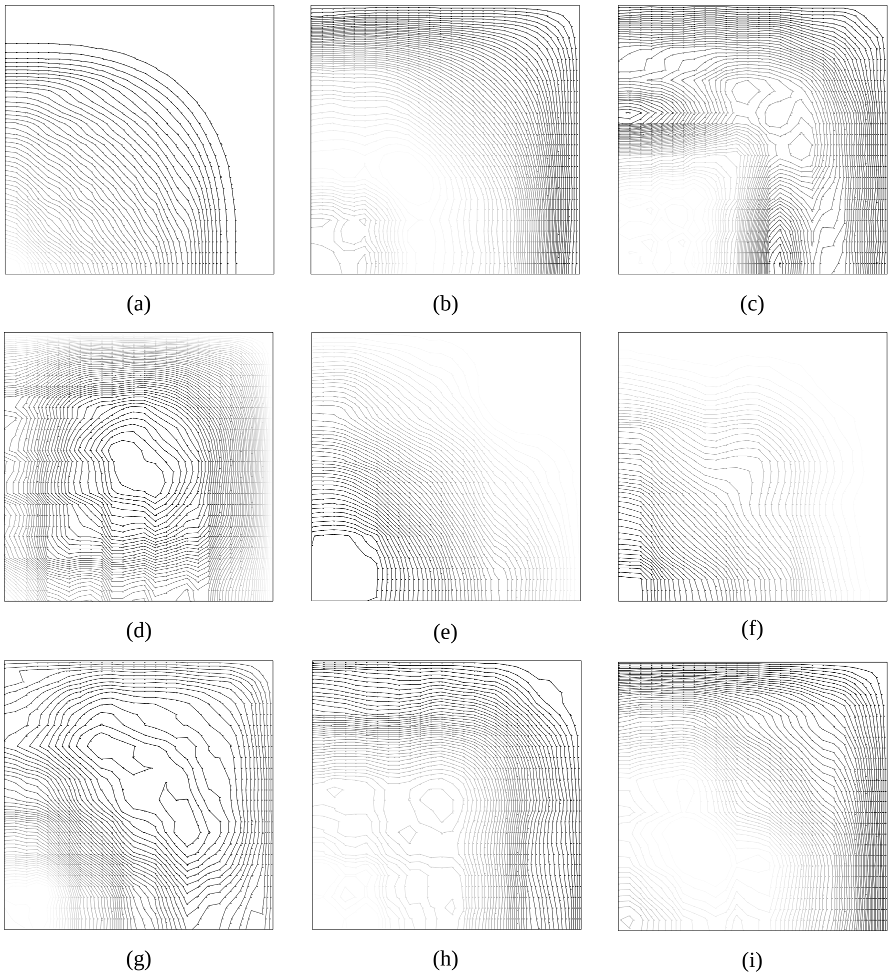

Figure 8: Computed fields at different instants of time, considering Δt = 0.02s (ϕ =1): (a) t = 0.22s; (b) t = 0.42s; (c) t = 0.62s; (d) t = 0.82s; (e) t = 1.02s; (f) t = 1.22s; (g) t = 1.42s; (h) t = 1.62s; (i) t = 1.82s.

4.3 Mass-spring model

In order to completely discuss the effectiveness of the new technique, it is also important to analyze the performance of its load operator matrix. In order to do so, consider an undamped SDOF model, with $w = 2\pi$, submitted to a load defined by $f(t) = \sin(t)$. For this model, displacement results are depicted in Fig. 9, considering the simplest load operator matrix discussed in section 3, i.e., $\beta_1 = \beta_3 = 1/2$ and

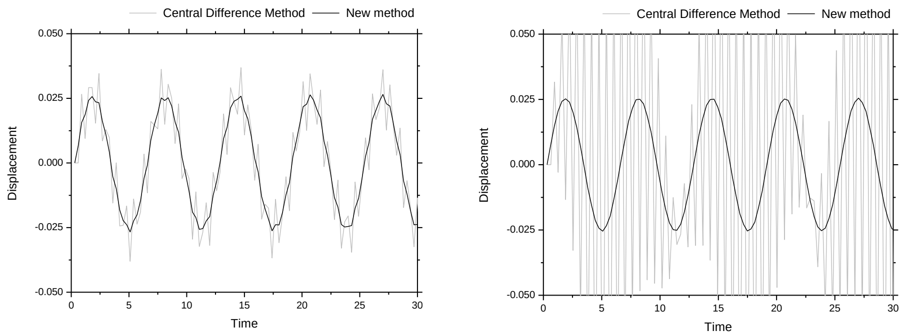

(a) (b)

Figure 9: Time history results for the loaded mass-spring model considering: (a) $\Delta t = 0.3\,s$; (b) $\Delta t = 0.318\,s$.

β_2= 0. Results are computed considering explicit conditionally stable techniques (i.e., the new technique with $a = 0$ and the CD) and time-steps close to their critical value (i.e., $\Delta t_{crit} = 1/\pi$). As one can notice, whereas in the CD strong oscillatory behaviour is observed in the results as the time-steps of the analyses get closer to their critical value, this oscillatory behaviour is not observed in the new method. These results illustrate once more the superior performance of the proposed technique.

Thus, not only the present technique is more accurate than the TR if implicit analyses are focused (in this case, $a = 0.25$ is suggested), but also it may be more accurate than the CD if explicit analyses ($a = 0$) are required.

5 Conclusions

In this work, a second-order time-marching procedure with enhanced accuracy is presented. The technique is based on selecting an α parameter lower than 1/2 (which characterizes the TR) and in a way that stability may be always ensured. Thus, the main features of the TR are retained (e.g., unconditional stability, no amplitude decay, no overshooting etc.) whereas accuracy is always improved, due to the reduction of period elongation errors (and due to an eventual selection of more accurate load operators, which is allowed by the new technique).

The new procedure is simple and easy to implement. It is efficient and, as the TR, requires no more than one set of implicit equations to be solved at each time step. Moreover, as described in section 2, the technique is truly self-starting, requiring no initial procedures at all. Thus, the proposed method is very competitive: it has no drawbacks compared to the TR (which is one of the most popular time-marching techniques), and it provides superior accuracy. In sections 3 and 4, numerical results are presented, illustrating the good performance of the methodology. Fig. 1(b) illustrates that the method is unconditionally stable, it introduces no amplitude decay and it always provides reduced period elongation errors, in comparison to the TR.

If explicit analyses are required, the new technique can also be more accurate than the CD (another extremely popular second-order time-marching technique), as it is illustrated in the third example. In this case, both methodologies are conditionally stable and have the same critical time-step value. Thus, the main features of the CD are retained, with enhanced accuracy being enabled due to richer load operators.

Acknowledgement: The financial support by CNPq (Conselho Nacional de Desenvolvimento Científico e Tecnológico) and FAPEMIG (Fundação de Amparo à Pesquisa do Estado de Minas Gerais) is greatly acknowledged.

References

Bathe, K. J. (1996): *Finite Element Procedures*. Prentice-Hall, Englewood Cliffs, NJ.

Bathe, K. J. (2007): Conserving Energy and Momentum in Nonlinear Dynamics: A Simple Implicit Time Integration Scheme. *Computers & Structures,* vol. 85, pp. 437–445.

Bathe, K. J.; Baig, M. M. I. (2005): On a composite implicit time integration procedure for nonlinear dynamics. *Computers & Structures,* vol. 83, pp. 2513–34.

Casadei, F.; Halleux, J. P. (2009): Binary spatial partitioning of the central-difference time integration scheme for explicit fast transient dynamics. *International Journal for Numerical Methods in Engineering,* vol. 78, pp. 1436–1473.

Chang, S. Y. (2010): A new family of explicit methods for linear structural dynamics. *Computers & Structures*, vol. 88, pp. 755–772.

Chung. J.; Hulbert, J. M. (1993): A time integration method for structural dynamics with improved numerical dissipation: the generalized α method. *Journal of Applied Mechanics*, vol. 30, pp. 371–375.

Clough, R. W.; Penzien, J. (1993): *Dynamics of Structures*, second ed. McGraw-Hill, New York.

Elgohary, T. A.; Dong, L.; Junkins, J. L.; Atluri, S. N. (2014a): Time domain inverse problems in nonlinear systems using collocation & radial basis functions. *CMES: Computer Modeling in Engineering & Sciences,* vol. 100, pp. 59–84.

Elgohary, T. A.; Dong, L.; Junkins, J. L.; Atluri, S. N. (2014b): A Simple, Fast, and Accurate Time-Integrator for Strongly Nonlinear Dynamical Systems. *CMES: Computer Modeling in Engineering & Sciences,* vol. 100, pp. 249–275.

Fung, T. C. (2002): Higher-order accurate time-step-integration algorithms by post-integration techniques. *International Journal for Numerical Methods in Engineering,* vol. 53, pp. 1175–1193.

Hughes, T. J. R. (2000): *The Finite Element Method.* Dover Publications INC, New York.

Hulbert, G. M.; Chung, J. (1996): Explicit time integration algorithms for structural dynamics with optimal numerical dissipation. *Computer Methods in Applied Mechanics and Engineering,* vol. 137, pp. 175–188.

Hulbert, G. M.; Jang, I. (1995): Automatic time step control algorithms for structural dynamics. *Computer Methods in Applied Mechanics and Engineering,* vol. 126, pp. 155–178.

Mancuso, M.; Ubertini, F. (2003): A methodology for the generation of low-cost higher-order methods for linear dynamics. *International Journal for Numerical Methods in Engineering,* vol. 56, pp. 1883–1912.

Mansur, W. J.; Soares, D.; Ferro, M. A. C. (2004): Initial conditions in frequency-domain analysis: the FEM applied to the scalar wave equation. *Journal of Sound and Vibration,* vol. 270, pp. 767–780.

Newmark, N. M. (1959): A method of computation for structural dynamics. *Journal Engineering Mechanics Division, ASCE,* vol. 85, pp. 67–94.

Rossi, D. F.; Ferreira, W. G.; Mansur, W. J.; Calenzani, A. F. G. (2014): A review of automatic time-stepping strategies on numerical time integration for structural dynamics analysis. *Engineering Structures,* vol. 80, pp. 118–136.

Smolinski, P. (1996): Subcycling integration with non-integer time steps for structural dynamics problems. *Computers & Structures,* vol. 59, pp. 273–281.

Soares, D. (2011): A new family of time marching procedures based on Green's function matrices. *Computers & Structures*, vol. 89, pp. 266–276.

Soares, D. (2015): A simple and effective new family of time marching procedures for dynamics. *Computer Methods in Applied Mechanics and Engineering,* vol. 283, pp. 1138–1166.

Soares, D.; Mansur, W. J. (2007): An efficient stabilized boundary element formulation for 2D time-domain acoustics and elastodynamics. *Computational Mechanics,* vol. 40, pp. 355–365.

Soares, D.; Mansur, W. J.; Lima, D. L. (2007): An explicit multi-level time-step algorithm to model the propagation of interacting acoustic-elastic waves using finite element / finite difference coupled procedures. *CMES: Computer Modeling in Engineering & Sciences*, vol. 17, pp. 19–34.

Tamma, K. K.; Namburu, R. R. (1990): A robust self-starting explicit computational methodology for structural dynamic applications: architecture and representations. *International Journal for Numerical Methods in Engineering,* vol. 29, pp. 1441–1454.

Tamma, K. K.; Zhou, X.; Sha, D. (2000): The time dimension: a theory towards the evolution, classification, characterization and design of computational algorithms for transient dynamic applications. *Archives of Computational Methods in Engineering,* vol. 7, pp. 67–286.